TU Delft

Delft University of Technology

Ship system design changes for the transition to hydrogen carriers

Van Rheenen, E.S.; Padding, J.T.; Kana, A.A.; Visser, K.

DOI
10.59490/imdc.2024.894

Publication date
2024

Document Version
Final published version

Published in
Proceedings of the 15th International Marine Design Conference (IMDC-2024)

Citation (APA)
Van Rheenen, E. S., Padding, J. T., Kana, A. A., & Visser, K. (2024). Ship system design changes for the transition to hydrogen carriers. In *Proceedings of the 15th International Marine Design Conference (IMDC-2024)* (International Marine Design Conference). TU Delft OPEN Publishing. https://doi.org/10.59490/imdc.2024.894

Important note
To cite this publication, please use the final published version (if applicable).
Please check the document version above.

Copyright
Other than for strictly personal use, it is not permitted to download, forward or distribute the text or part of it, without the consent of the author(s) and/or copyright holder(s), unless the work is under an open content license such as Creative Commons.

Takedown policy
Please contact us and provide details if you believe this document breaches copyrights.
We will remove access to the work immediately and investigate your claim.

This work is downloaded from Delft University of Technology.
For technical reasons the number of authors shown on this cover page is limited to a maximum of 10.

Proceedings of 15th International Marine Design Conference (IMDC-2024)
June 2-6, 2024
Amsterdam, the Netherlands

Ship system design changes for the transition to hydrogen carriers

E.S. van Rheenen[1,*], J.T. Padding[2], A.A. Kana[1] and K. Visser[1]

ABSTRACT

Reducing the use of fossil fuels in shipping requires new, alternative maritime fuels. Hydrogen carriers offer a safe and energy-dense solution for storing hydrogen, a zero-emission alternative fuel. This research focuses on ammonia borane, $NaBH_4$, n-ethylcarbazole and dibenzyltoluene. Applying hydrogen carriers influences ship design significantly, as they require additional specialised equipment to remove hydrogen from the hydrogen carrier. This research estimates the size of the equipment. As this equipment will need to be stored and maintained on the ship, the exact sizing and sequence of the additional equipment will likely influence ship design. Results show that the reactor size is significant for all hydrogen carriers. The mixing tank is considerably sized for $NaBH_4$ and ammonia borane, while the heat exchangers are large for dibenzyltoluene and n-ethylcarbazole.

KEY WORDS

Hydrogen carriers; Heat exchangers; Dehydrogenation; Solid hydrogen carrier; LOHC

INTRODUCTION

Reducing fossil fuels in shipping requires new, alternative maritime fuels. However, applying alternative power sources can have significant implications for ship design and is thus extensively researched, mainly focusing on using ammonia or methanol as alternative fuel (Pawling et al., 2022; Souflis-Rigas et al., 2023; de Vos et al., 2022). Hydrogen is another of these alternative fuels, but it has a low volumetric energy density. Hydrogen carriers offer a safe and energy-dense solution for storing hydrogen, a zero-emission alternative fuel (van Rheenen, Padding, Slootweg, & Visser, 2023). Using hydrogen carriers will significantly influence the ship's power plant and, consequently, ship design, as additional components such as hydrogen release reactors are required. Additionally, these reactors cannot be placed everywhere on the ship, as they produce pure hydrogen and thus need to be in regulated and well-ventilated spaces. Besides the reactor, more components, such as heat exchangers, may be necessary. All these additional components that are required to release hydrogen from hydrogen carriers are components that are not necessary without hydrogen carriers. So, using hydrogen carriers may result in more components and, thus, more complexity.

As these additional components are of unknown size, it is unclear whether they are significantly sized to influence ship design. For other alternative fuels, such as methanol or LNG, it is clear that the additional components will influence ship design (Souflis-Rigas et al., 2023; de Vos et al., 2022). Research focuses on resulting required design changes because of the space other components take up (Souflis-Rigas et al., 2023; de Vos et al., 2022). However, the number of components

[1] Department of Maritime and Transport Technology, Delft University of Technology, Delft, the Netherlands
[2] Department of Process and Energy, Delft University of Technology, Delft, the Netherlands;
[*] Corresponding Author: E.S.vanRheenen@tudelft.nl

Submitted: 23 February 2024, Revised: 22 April 2024, Accepted: 1 May 2024, Published: 23 May 2024
©2024 published by TU Delft OPEN Publishing on behalf of the authors. This work is licensed under CC-BY-4.0.
Conference paper, DOI: https://doi.org/10.59490/imdc.2024.894 e-ISSN: 3050-4864

explicitly needed for hydrogen carriers as power sources, and the size of these specific components are unknown. The sequence, size, and number of this specialised hydrogen carrier equipment are required to see how they influence and perhaps limit ship design.

Our previous research identified a promising set of hydrogen carriers for use as alternative fuels on ships (van Rheenen, Padding, Slootweg, & Visser, 2023). The most promising ones were sodium borohydride ($NaBH_4$), potassium borohydride (KBH_4), ammonia borane (NH_3BH_3), n-ethylcarbazole (NEC), and dibenzyltoluene (DBT). Next, we developed a 0D thermodynamic model to evaluate the effective energy density of these hydrogen carriers in combination with various energy converters (van Rheenen, Padding, & Visser, 2023). The energy converters were a proton exchange fuel cell (PEMFC), solid oxide fuel cell (SOFC), hydrogen-powered internal combustion engine (ICE) and gas turbine (GT). Integration of the carrier with the energy converter is crucial to calculate the overall energy density. Heat integration can minimise losses, particularly for DBT and NEC, which require heat during the hydrogen release process. Findings from the model suggest that these hydrogen carriers hold significant promise as alternative fuels. However, the 0D model does not account for geometrical parameters or the ship's sizing restrictions.

Thus, this paper aims to identify and size the relevant components when using the hydrogen carriers mentioned earlier as power sources onboard ships. First, all the required components for each hydrogen carrier must be known. Only the specifically relevant components for hydrogen carriers are considered; general equipment for hydrogen-fueled ships is not regarded. Each of these components will then be sized. This will form a first step in designing hydrogen carrier-powered ships.

BACKGROUND

Sodiumborohydride, ammonia borane, N-ethylcarbazole and dibenzyltoluene are considered in this research. Table 1 gives an overview of the relevant parameters of these hydrogen carriers. As energy converters, same as in the previous model, the ICE, GT, PEMFC and SOFC are considered (van Rheenen, Padding, & Visser, 2023).

Hydrogen carriers

The hydrogen carriers will be divided into endothermic and exothermic release hydrogen carriers. Within these groups, the processes and, thus, the required equipment are very similar. The phase, energy density and energy requirements are also similar. All processes occur at relatively low pressures, around 1 to 10 bars; thus, specialised high-pressure equipment is unnecessary.

Endothermic release

The endothermic release hydrogen carriers are NEC and DBT. Both are liquid organic hydrogen carriers (LOHCs). The release mechanism for the LOHCs is very similar and is as follows:

$$\mathrm{LOHC}^{+} + \mathrm{Energy} \rightarrow \mathrm{LOHC}^{-} + n\mathrm{H}_2 \tag{1}$$

The significant difference is the temperatures at which they react and the heat required for dehydrogenation. DBT's dehydrogenation temperature lies between 553 and 593K; temperatures above 573K are required to reach full dehydrogenation, while DBT will start dissociating at temperatures above 563K. A temperature of 573K is chosen in the model, as this temperature is often used in experiments, and full dehydrogenation can be achieved without compromising the fluid too much (Asif et al., 2021). The dehydrogenation process requires 558 kJ/mol of full LOHC (Niermann et al., 2019). The dehydrogenation temperature for NEC lies between 453 and 523K. The dehydrogenation process is much slower at lower temperatures. The model uses a temperature of 503K. The dehydrogenation process is fast at this temperature, without having

Table 1: Parameters of hydrogen carriers

Parameter	DBT	NEC	$NaBH_4$	Ammonia borane
Theoretical energy density [MJ/kg]	7.44	6.98	25.56	23.52
Theoretical energy density [MJ/L]	7.0	6.63	27.34	14.4
Hydrogen yield per molecule of hydrogen carrier [mol/mol]	9	6	4	3
Molecular weight [g/mol]	290.54	207	37.8	30.8
Heat capacity fuel (incl. water if necessary [kJ/kgK]	1.96	2.04	4.54*	4.54*
Heat capacity spent fuel [kJ/kgK]	1.82	1.56	N.R.	N.R.
Dehydrogenation temperature [K]	573	503	353	353*
Dehydrogenation energy [kJ/mol Fuel]	558	318	-210	-156
Sources	(Lee et al., 2021) (Kwak et al., 2021)	(Stark et al., 2015) (Müller et al., 2015) (Teichmann et al., 2012)	(Zhang et al., 2006) (Kojima, 2019) (Ye et al., 2020)	(Sanyal et al., 2003) (Chandra & Xu, 2007)

Values denoted with * are estimated by the authors combined with data from Aspen as no precise information was available.
N.R. stands for 'Not required' as these values are not required in this calculation. When a solution is mixed, the heat capacity of the sol

high heating loads (Brückner et al., 2014). The hydrogenation process requires 318 kJ/mol of full LOHC (Niermann et al., 2019). van Rheenen, Padding, and Visser (2023) showed that, with an essential integration, a large part of the required heat could be supplied by the energy converter and heat available in the spent fuel, with similar results found by Preuster et al. (2018), who looked at a specific hydrogen carrier and energy converter. Figure 1 gives an overview of the specific components required for the hydrogen carrier to release hydrogen. After the carrier is transported from the tank, heat exchangers are used to preheat the carrier up to the dehydrogenation temperature. Part of this heat exchange already has to occur in the tank, as DBT is highly viscous; thus, preheating is required to get it out of the tank.

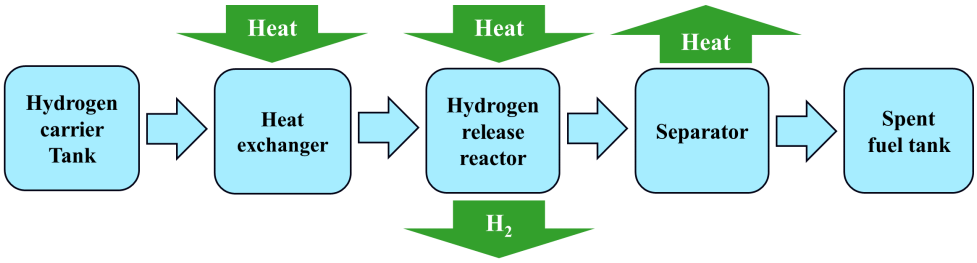

Figure 1: Simplified flow diagram with required components and main heat and mass flows for endothermic release hydrogen carriers

Exothermic release

Ammonia borane and $NaBH_4$ release hydrogen exothermically upon reacting with water, according to the following equations:

$$NaBH_4 + (2 + x)H_2O \rightarrow 4H_2 + NaBO_2.xH_2O \tag{2}$$

$$NH_3BH_3 + 3H_2O \rightarrow 3H_2 + B(OH)_3 + NH_3 \tag{3}$$

These reactions are similar, requiring water and releasing equally or more hydrogen than initially stored in the molecule, as the process also releases hydrogen within the water molecules. The boron-based spent fuel is also very similar. Regeneration of this spent fuel to the original molecule is possible but energy intensive due to the strong B-O bonds (Stephens et al., 2007). The exact composition of the spent fuel of $NaBH_4$ (equation 2) depends on the temperature of the reaction. At the optimal reaction temperatures of 333 to 353K, the composition is $NaBO_2.2H_2O$.

Equation 3 shows the release mechanism of ammonia borane, which produces hydrogen and ammonia. Ammonia gas can be burned in a heat engine, for example, in a dual-fuel ammonia-hydrogen internal combustion engine. Additionally, it can be decomposed into N_2 and H_2, after which the H_2 can be used in a fuel cell. Finally, ammonia gas can be stored on board. Storage is not considered feasible because of the required safety regulations and additional space. The decomposition process is also disregarded, as this process is highly energy-intensive. Thus, in this study, similar to in van Rheenen, Padding, and Visser (2023), only dual-fuel options of ammonia and hydrogen gas are considered. Only the PEMFC cannot run on the ammonia-hydrogen dual-fuel of the four investigated energy converters.

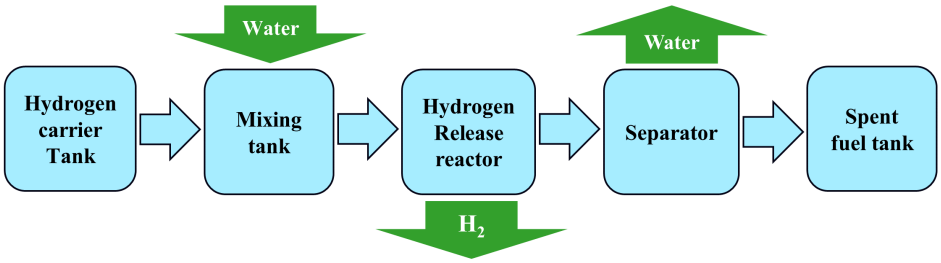

Figure 2: Simplified flow diagram with required components and main heat and mass flows for exothermic release hydrogen carriers

Energy converter

Energy converters convert the chemical energy inside hydrogen to electrical or mechanical energy. The model will simulate four different energy converters, namely a hydrogen spark ignition (SI) ICE, a PEMFC, SOFC and GT, as these are all considered possible alternatives within the shipping sector. At the moment, a compression ignition running on pure hydrogen is not feasible without a way to ignite the hydrogen and is thus not regarded (Dimitriou & Tsujimura, 2017). Additionally, SI ICEs are more researched, and more data is available for these heat engines (Wang et al., 2019). The output of both the SI ICE and GT is regarded as mechanical. Both are assumed to be able to run on pure hydrogen and a hydrogen-ammonia mixture (Gohary & Seddiek, 2013; Rosado et al., 2019; Wang et al., 2019).

Table 2: Parameters of energy converters, including sources.

Parameter	SI-ICE	PEMFC	SOFC	GT
T coolant [K]	363	348	-	-
P coolant [%]	30	44.8	0	0
P effective [%]	35	42.9	48	37.5
T flue gas [K]	623*	-	1023	790
P flue gas [%]	25	0	42.1	53
P losses [%]	10	12.3	9.9	9.5
Sources	(Wang et al., 2019)	(Zhao et al., 2017)	(van Veldhuizen et al., 2023)	(Gohary & Seddiek, 2013) (Rosado et al., 2019)

P is the percentage of overall power distribution, mainly based on Sankey diagrams. * Flue gas temperature of SI-ICE largely fluctuates depending on operating conditions and can range from 423 to 773K

METHOD

Using hydrogen carriers on ships results in additional components needed on board compared to using pure hydrogen or conventional fuels. Some of these components are specific to hydrogen carriers, whereas other components, such as the energy converter, may be different for hydrogen-based fuels in general. This research only covers the hydrogen carrier-specific components, not the hydrogen-specific components. These components are visible in figure 3, where the components that will be looked at in detail in this research are coloured green. The required input parameters, such as mass flows, compositions and temperatures, are calculated using the 0D model we previously created (van Rheenen, Padding, & Visser, 2023). Figure 4 shows a simplified model outline based on van Rheenen, Padding, and Visser (2023). The model is built so that each energy converter, regardless of the hydrogen carrier, will always have an output power of 2 MW, which is relevant for medium-sized vessels such as ferries and small cargo ships.

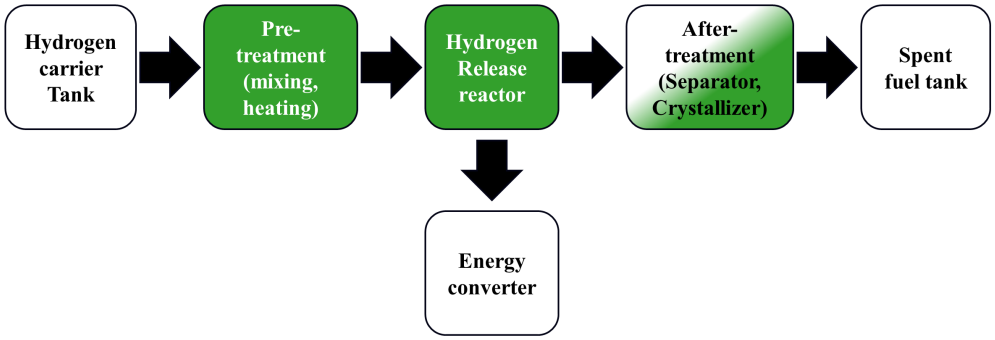

Figure 3: Overview of all components required on a ship when using hydrogen carriers as a power source. The components denoted in green are hydrogen carrier specific components and, thus, the main focus of this research

This section describes the necessary steps to upgrade them to get an overview of the sizing. A different approach is used for each component due to their significant difference in functionality. The parameters required for upgrading the components, such as mass flows and temperatures, are given by the 0D model. The following subsections will describe each critical component in detail and how they can be upgraded.

0D Model

Figure 4 gives an overview of the 0D thermodynamic model's layout, as implemented in Matlab Simulink. The power requirement, the hydrogen carrier and the energy converter can be chosen. These three parameters then define the mass flow of the hydrogen carrier. This mass flow, in its turn, defines the required energy for preheating and, if applicable, dehydrogenation. The model runs a complete iteration, including an energy balance check, and adjusts the mass flow accordingly if the required power and the output power do not match.

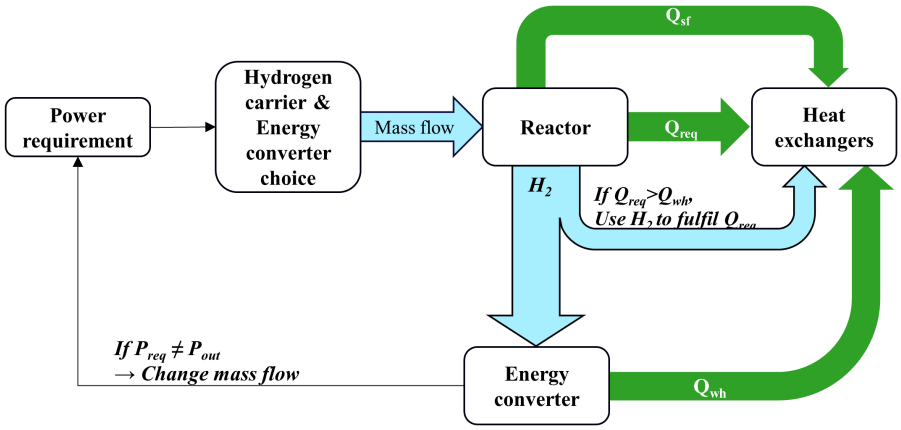

Figure 4: Simplified overview model. Flows that are used as a heat source can be turned on and turned off when necessary. Q_{wh} stands for waste heat, Q_{req} is the heat required for preheating and, if applicable, dehydrogenation and Q_{sf} stands for the heat inside the spent fuel

Tables 1 and 2 give an overview of the used parameters and the resources from which they were derived. The thermodynamic model provides estimates and a simplified representation of reality. For example, the model does not consider the preheating of air for a SOFC. In reality, this preheating, which is required, is a major, high-temperature heat sink (van Veldhuizen et al., 2023). When the heat needed for the dehydrogenation of the hydrogen carrier cannot be covered with waste heat from the energy converter, hydrogen will have to be burnt to cover the heat requirement. The heat required for preheating and dehydrogenation, Q_{req}, and the heat available inside the spent fuel, Q_{sf}, are calculated according to the following equation:

$$\dot{Q} = \dot{m} \cdot c_p \cdot \Delta T \tag{4}$$

With $\dot{Q}$ the heat in kW, $\dot{m}$ the mass flow in kg/s, c_p the heat capacity, in kJ/kgK and ΔT the temperature difference in Kelvin. In the Matlab model, c_p is considered constant, not temperature-dependent. Q_{wh} is defined by the percentage of heat going from the reactor to heat losses (denoted by P coolant and P flue gas in table 2). A fixed temperature difference is set for flue gasses and coolant, which is used to calculate the flue gas's or coolant's mass flow, using equation 4. The required mass flow of the flue gas or coolant to go into the heat exchanger is similarly calculated. However, if the heat (denoted by Q) is larger than required to heat the hydrogen carrier in that temperature window, the mass flow is adjusted, as equation 4 is always true (Cengel & Ghajar, 2014).

Pretreatment: mixing tank

The boron-based hydrogen carriers are mixed with water in the mixing tank. This mixture is then further heated in heat exchangers before entering the reactor. The mixing tank uses a stirrer. The size of the mixing chamber depends on the required power and the selection of spent fuel. The hydrolysis reaction of the boron-based carriers is visible in equation 2 and 3. The hydrolysis requires a surplus of water. The amount of water, defined by the (2+x) term, is the minimum amount

needed for the reaction to happen. Additionally, it defines the composition of the spent fuel. The (2+x) term depends on the temperature if enough water is available (Andrieux et al., 2012). More important, however, is the solubility of the fuel and spent fuel in water. The amount of water should be sufficient to avoid spontaneous crystallisation, which may result in clogging. For both ammonia borane and sodium borohydride, the spent fuel is less soluble in water than the fuel. As both the fuel and spent fuel are present in the reactor, the limiting substance defines the amount of water. For ammonia borane and its spent fuel product, boric acid, the limit at temperatures of 353K is about 19 wt% of ammonia borane in water (Crapse & Kyser, 2011). For sodium borohydride, this limit lies at around 44 wt% sodium borohydride in water (Andrieux et al., 2012). These limits thus define the minimum amount of water required in the mixing tank.

The size of the mixing tank is determined as follows. The amount of water required for the boron-based hydrogen carrier spent fuel to completely dissolve at 353K (the operating temperature of the reactor) is calculated. This amount of water is compared to the stoichiometric amount of water required for the reactions (as depicted in equations 2 and 3). The largest amount of water is taken. This amount should always be compared to the amount of boron-based hydrogen carrier that can be dissolved at room temperature (293K) without crystallisation (Demirci, 2020; Haynes, 2011). The spent fuel is the limiting factor for sodium borohydride and ammonia borane. The largest amount of water (stoichiometric or dissolvent value) must be held in the mixing tank. As the boron-based hydrogen carriers will completely dissolve, their volume is negligible.

Pretreatment: heat exchangers

All hydrogen carriers need to be heated before entering the reactor. The amount and type of heat exchangers depend on the energy converter chosen and the hydrogen carrier.

A heat exchanger with a large heat transfer surface per unit volume is a compact heat exchanger. The ratio of heat transfer surface area to the volume of the heat exchanger is called the area density, denoted with β(Cengel & Ghajar, 2014). Generally speaking, heat exchangers with a β in excess of 700 m^2/m^3 are classified as compact, with heat exchangers in microreactors reaching area densities of over 15000 m^2/m^3 (Cengel & Ghajar, 2014; Reay, Ramshaw, & Harvey, 2008). However, these high-area density heat exchangers, which also include printed circuit heat exchangers, have high pressure drops, making them less suitable for the specific applications addressed in this paper due to the high viscosity of some of the fluids, such as LOHCs (Cengel & Ghajar, 2014). To have an efficient heat exchanger, the thermal conductance of both fluids should be similar (Shah & Sekulić, 2003). This is more likely the case for liquids than for liquid-gas heat exchangers. Thus, liquid-liquid heat exchangers generally require different heat exchangers compared to liquid-gas heat exchangers (Shah & Sekulić, 2003).

The type of heat exchanger is defined by the fluids flowing through it. Generally, heat exchangers can differ depending on the fluid (gas or liquid), viscosity, fouling, pressure and temperature of the fluid (Cengel & Ghajar, 2014; Shah & Sekulić, 2003). As the pressures are similar for all four hydrogen carriers (1-10bars), different heat exchangers are unlikely to be required based on pressures. Fluid types differ, and both liquid-liquid and gas-liquid heat exchangers are required. Similarly, the temperature ranges of the hydrogen carriers vary significantly, as dehydrogenation temperatures range from 353K to 573K. Finally, the viscosity of the different hydrogen carriers differs. The boron-based hydrogen carriers are mixed with water, and these mixtures have viscosities that are relatively similar to water. Dibenzyltoluene is highly viscous at low temperatures, with viscosities of up to 4000 mPas (Müller et al., 2015).

Additionally, several other parameters must be known to evaluate the sizing of heat exchangers, namely, the mass flows, and in- and outlet temperatures of both the hot and cold sides. Thus, the 0D model should provide these mass flows. However, the 0D model uses a fixed heat capacity to calculate the mass flows of the hot side, which may result in small errors. The heat exchangers will all be designed in Aspen Exchanger Design & Rating (EDR), which will adjust the mass flow of the hot fluid when necessary. Aspen EDR can calculate the exact size and mass of heat exchangers and is widely used in industry and heat exchanger design research (K. Hooman, personal communication, November 27 2023). As a basis, the material properties from Aspen are incorporated. When a disagreement occurs between data obtained from any of the Aspen databases and experimental values from the literature, the data from the literature is taken. As the 0D model only incorporates a fixed, heat capacity value, the heat exchanged within a heat exchanger might differ between Aspen and the 0D

model. In these cases, the mass flow of the heat source is adjusted accordingly while checking if the mass flow does not exceed the maximum mass flow according to equation 4.

Expected amount and sequence of heat exchangers

Because we used the 0D model before, we can estimate the amount and sequence of the heat exchangers (van Rheenen, Padding, & Visser, 2023). The boron-based hydrogen carriers are mixed with water before entering the release reactor. This mixture has to be heated as well, and considering the difficulty of heating solid powders, the boron-based hydrogen carriers will be heated as a mixture. Heating the mixture will occur in a heat exchanger and requires only one heat exchanger, as they need to be heated to only 353K. No heat exchangers with spent fuel are used to avoid crystallisation inside heat exchangers. So, either flue gasses or coolant is used to preheat the exothermic-release hydrogen carriers, which are believed to contain enough heat to fulfil the requirements.

The endothermic-release hydrogen carriers, the LOHCs, will likely need more heat exchangers. When applicable, the LOHC will be heated in the first heat exchanger using the coolant from the energy converter. The second heat exchanger uses the spent fuel to heat the LOHC to almost the dehydrogenation temperature. A drawback for NEC here is that its spent fuel turns into a solid at temperatures lower than 343K. Thus, the fuel must be heated to at least 343K before entering the second heat exchanger. Finally, using flue gasses, a third heat exchanger will heat the LOHC until it reaches the dehydrogenation temperature.

After treatment: separator and crystallizer

If the conversion rate of the LOHC is below 100%, a separator may be advantageous. The threshold below which a separator becomes worthwhile depends on the energy density, desired ship range, and volumetric fuel tank requirements. However, if a separator is larger than the additional fuel required to compensate for the lower conversion efficiency, it would not be worth using.

Next to the separator, a crystalliser can crystallise the spent fuel from the water to avoid storing large amounts of spent fuel. This water prevents the spent fuel from crystallising and thus clogging the system. The water required depends on the spent fuel, as the solubility of the spent fuel is lower than that of the fuel itself (Andrieux et al., 2012; Sanyal et al., 2003; Crapse & Kyser, 2011). However, the water also adds a large amount of weight and volume to the spent fuel, reducing the energy density of the whole system. Thus, crystallising the spent fuel is essential, and a crystalliser has to be added to the system. For hydrogen carriers that exothermically release hydrogen, such as sodium borohydride and ammonia borane, the crystalliser's size must be at least as big as the reactor's. In an emergency, the content of the reactor can then be dumped in the cooled crystalliser to stop or at least significantly slow down the hydrogen release reaction. This is unnecessary for hydrogen carriers that release endothermically as withholding heat will stop the reaction.

The sizing of the crystalliser and the separator highly depends on the conversion rate inside the reactor. In turn, this depends on the choice of catalyst, the amount of catalyst, the temperature, the throughput time of the reactor and, for boron-based carriers, the amount of additional water. Especially the catalyst choice is of significant influence and is thus well-researched (Abdelhamid, 2021). Because of the depth of the studies on this subject, it was decided not to incorporate this.

Release reactor

The hydrogen release reactor is where the hydrogen is released from the hydrogen carrier. In this reactor, the hydrogen carrier passes by the catalysts, upon which it reacts and releases hydrogen. Many researchers are studying this process. We refer to Fogler (2016) for more detailed information on release reactors. In this work, however, the release reactor will be modelled as a plug flow reactor, with a jacket around it to provide the necessary heat or cold. The plug flow reactor is as-

sumed to have a membrane to remove the hydrogen. The hydrogen gas will expand vastly and thus significantly influence the reactor's working if not removed immediately.

The dehydrogenation of endothermic-release hydrogen carriers requires heat. A buffer fluid will be used when the heat has to be supplied to the reactor, and the heat source is not considered constant (such as flue gasses). This buffer fluid reduces the system's efficiency but controls the heating system. Using a buffer fluid can prevent overheating of the reactor, which can result in the decomposition of the hydrogen carrier and has to be avoided.

RESULTS AND DISCUSSION

This section discusses the main results. The model is first validated using pinch diagrams and a sensitivity analysis. The sizing of the mixing tank and reactor, as well as the type and sizing of the heat exchangers, is discussed next. It is important to realise that only the components from figure 3 are considered. The storage tanks, engines or fuel cells, and potential hydrogen burners are not considered, despite taking up significant amounts of space. The PEMFC is not considered in the case of ammonia borane. Ammonia borane releases both hydrogen and ammonia. Cracking or storage of ammonia is not deemed feasible and the ammonia will be used as fuel, together with hydrogen (van Rheenen, Padding, & Visser, 2023). This rules out a PEMFC, as ammonia is toxic to PEMFCs and strongly reduces the performance of the PEMFC (Halseid, Vie, & Tunold, 2006). Thus, the figures of ammonia borane will have only three results and the PEMFC is left out.

Validation

The model is validated in multiple ways. Pinch diagrams are used to check whether the heat flows from the 0D model are thermodynamically possible. A sensitivity analysis provides information on the influence of the viscosity on the size of a heat exchanger.

Pinch diagrams

Pinch diagrams are used to validate the results. Pinch diagrams show whether heat exchangers comply with the second law of thermodynamics and also where the design is most constrained. Heat exchangers will correctly transfer heat if the lines representing the hot fluid stay above the lines representing the cold fluid at all times; crossing lines means that the exchanger does not comply with the second law. The design is most constrained at the location where the hot and cold lines are closest, the 'pinch' (Kemp & Shiun Lim, 2020).

Figure 5 gives an overview of four of the pinch diagrams generated by the 0D model. As there are no crossing lines, the required heat exchangers all comply with the second law of thermodynamics. The figures, however, do show interesting differences. Figure 5a is an example of what all pinch diagrams look like for both $NaBH_4$ and ammonia borane: two straight lines, with a sufficiently significant temperature difference (at least 10 K or more). The lines are straight because the mass flow of the flue gas is calculated following the temperature and heat demand: it is less than the total mass flow of the flue gas. Mass flows are more straightforward to regulate than temperatures and lower mass flows require smaller heat exchangers.

Figure 5b gives an overview of an endothermic-release hydrogen carrier, DBT, combined with an ICE. The flue gas of the ICE does not contain sufficient heat to cover the heating demand of the dehydrogenation reactor. Hence, additional heat by burning hydrogen is required. Similarly, figure 5c shows that combining a PEMFC and DBT will result in hydrogen burning necessary for heating and dehydrogenation. The hydrogen used for burning is a loss, as it is first released from DBT but cannot be used for power. This combination is thus unfavourable. Finally, figure 5d shows the combination of NEC and a gas turbine. No additional heat is required as the flue gas (HT) line covers the whole dehydrogenation. Thus, no hydrogen has to be burned. As the spent fuel of NEC is solid at temperatures lower than approximately 343K, the preheating of the

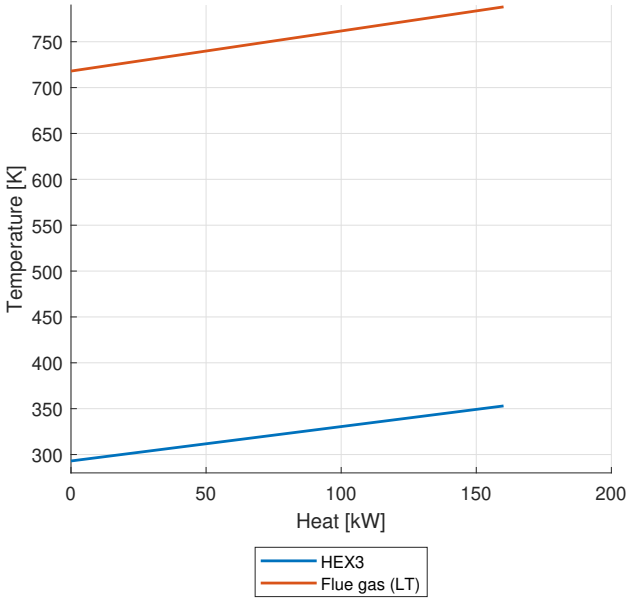

(a) Pinch diagram of $NaBH_4$ combined with an SOFC

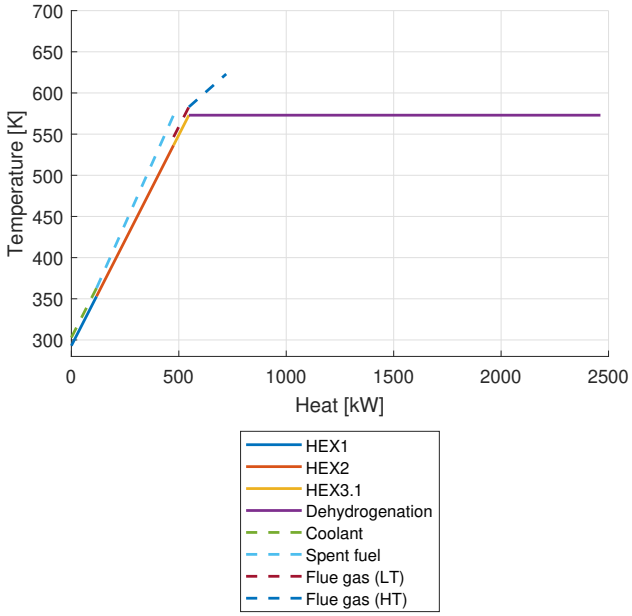

(b) Pinch diagram of DBT combined with an H2-ICE

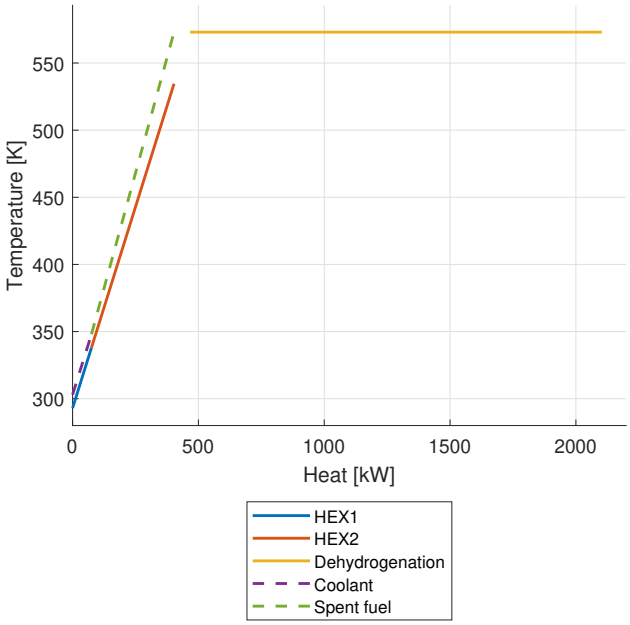

(c) Pinch diagram of DBT combined with a PEMFC

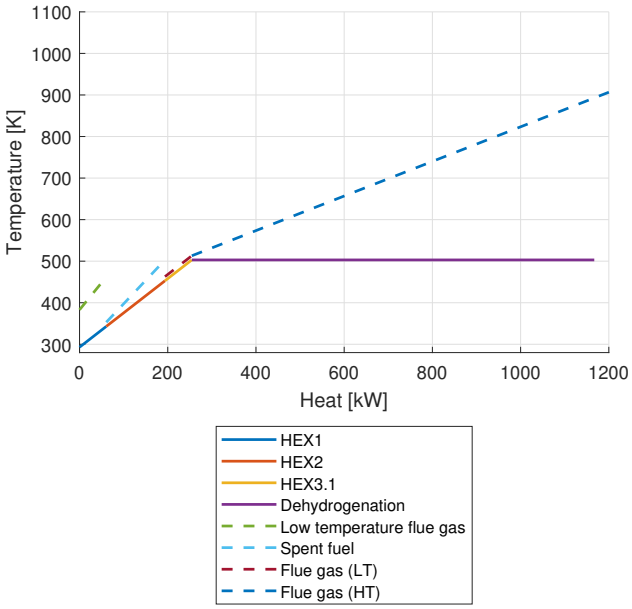

(d) Pinch diagram of NEC combined with a GT

Figure 5: Pinch diagrams for a selected group of hydrogen carriers and energy converters

fuel is done using low-temperature flue gas. This flue gas is not cooled below 373K to avoid condensation in the heat exchanger.

Validation: Influence of viscosity

The viscosity of ammonia borane mixed with water is unknown. Thus, we made an estimation. The level of ammonia borane in the water (3mol/L, (Crapse & Kyser, 2011)) is much lower than the solubility limit. Therefore, low viscosity (1-2 mPas) is assumed. A sensitivity analysis was used to control the influence of small changes in the viscosity on the output of Aspen EDR. The viscosity was changed with a factor of 1.5 and 2, without any changes in the heat exchanger. Thus, such small changes in viscosity are insignificant.

Mixing tank

To estimate the size of the mixing tank, the residence time and the mass flow of the mixture must be known. The residence time is defined by the dissolution time of the crystals, and is strongly influenced by the mixing equipment. The residence time should be sufficient to ensure sufficient mixing to avoid crystallisation. The residence time in mixing vessels for sodium borohydride and ammonia borane is estimated to be relatively short (about 3 minutes), resulting in small mixing tanks. The mixing time is based on data from Aspen for $NaBH_4$. The same mixing time for ammonia borane is taken, as no additional data is available for ammonia borane. Experiments should be performed on the mixing time to estimate the mixing tank size better. Figure 6 gives an overview of the mixing tank size without considering a safety factor.

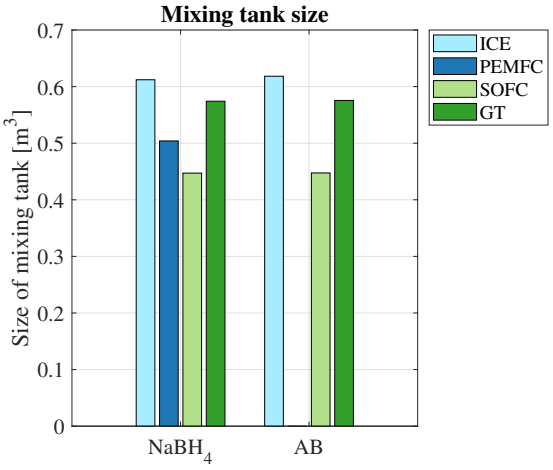

Figure 6: Size of mixing tanks, without safety factor

Heat Exchangers

This section will describe the choice and consequent size of heat exchangers.Table 3 gives an overview of the types of heat exchangers required for the different hydrogen carrier and energy converter combinations.

Choice of heat exchangers

Two main types of liquid-liquid heat exchangers exist: the shell-and-tube heat exchanger and the plate heat exchanger. The shell-and-tube heat exchanger is very common in industrial heat exchangers but is less suitable for the specific applications onboard ships, as they are relatively large and heavy (Cengel & Ghajar, 2014; Shah & Sekulić, 2003). This thus leaves plate

Cold medium	Hot medium	Mediums	Heat exchanger type	Sizing (Order of magnitude)
$NaBH_4$ and NH_3BH_3	Coolant	Liquid-Liquid	Plate	$8 \cdot 10^{-3}$ m^3
$NaBH_4$ and NH_3BH_3	Spent fuel	Liquid-Liquid	Avoided due to crystallisation resulting in possible clogging	N.A.
$NaBH_4$ and NH_3BH_3	Flue gas	Liquid-gas	Plate with fins	$5 \cdot 10^{-3}$ m^3
LOHCs	Coolant	Liquid-Liquid	Plate	$5 \cdot 10^{-3}$ m^3
LOHCs	Spent fuel	Liquid-Liquid	Plate	$8 \cdot 10^{-3}$ m^3
LOHCs	Flue gas (Preheat)	Liquid-gas	Plate with fins	$1 \cdot 10^{-3}$ m^3
Heat transfer fluid	Flue gas	Liquid-gas	Plate with fins	1 m^3
LOHC (dehydrogenation)	Heat transfer fluid	Liquid-Liquid	Jacketed reactor	4 m^3

Table 3: Summary heat exchangers and reactor types and sizes

heat exchangers, which are well suited for liquid-to-liquid heat exchange applications. The main limitation of plate heat exchangers is their unsuitability when large pressure or temperature differences between the hot and cold fluids occur (Cengel & Ghajar, 2014; Shah & Sekulić, 2003). Neither occurs in any of the heat exchangers. Plate heat exchangers are generally cheaper, have less fouling and have shorter residence times than shell and tube heat exchangers (Shah & Sekulić, 2003). As the dehydrogenation processes for all of the mentioned hydrogen carriers occur at only a few bars, and coolants are generally in a similar pressure range, this does not seem to be an issue. Thus, plate heat exchangers are the only type of heat exchangers considered in this research for liquid-to-liquid use.

The only exception to the plate heat exchangers is dehydrogenation reactors' heating (and cooling). The reactor design focuses on the reactor itself and less on the heating or cooling. For simplicity, a jacketed reactor is chosen. The jacket around the reactor can provide necessary heating or cooling. The reactors will be considered plug flow reactors, and the hydrogen is assumed to be immediately removed from the reactor. This latter is required as hydrogen is a gas and takes up a lot of volume. Removing hydrogen gas as soon as possible is essential for the reactor to keep working properly.

For liquid-gas use, plates with fins heat exchangers are used. A sensitivity analysis showed that plate heat exchangers would be significantly larger than plate-with-fins heat exchangers. Plate with fin heat exchangers are often used for liquid-gas heat exchangers, as they can have different surface areas for the gas and the liquid. Gasses usually require larger surface areas due to their lower heat capacities.

Table 3 gives an overview of the types of heat exchangers chosen for each combination of cold and hot fluids, including the type of fluid and the resulting order of magnitude.

Sizing of heat exchangers

Figure 7 gives a more in-depth overview of the sizes of the different heat exchangers. Clear differences between the boron-based hydrogen carriers and the LOHCs can be seen. The LOHCs require several heat exchangers, which are significantly sized, while the boron-based hydrogen carriers require a single, small heat exchanger with a size of several litres. Between the boron-based carriers, the heat exchangers required for heating sodium borohydride (represented in figure 7c) are smaller than those for ammonia borane (figure 7d). This difference is explained by the different amounts of water required for these carriers. Due to the higher solubility limits of the spent fuel of sodium borohydride, less water is required in the process. More water is required in the process for ammonia borane, resulting in a larger overall mass flow, greater heat demand and thus, a larger heat exchanger. These figures also show that heat exchangers that use hot gasses as heat sources can be smaller than liquid-liquid heat exchangers. The internal area of the plate with fins heat exchanger is larger than that of the plate heat exchangers.

The results of the heat exchanger geometry for liquid organic hydrogen carriers differ greatly. The heat exchangers are generally tenfold larger than those of the boron-based hydrogen carriers. From figures 7a and 7b, it appears that the heat ex-

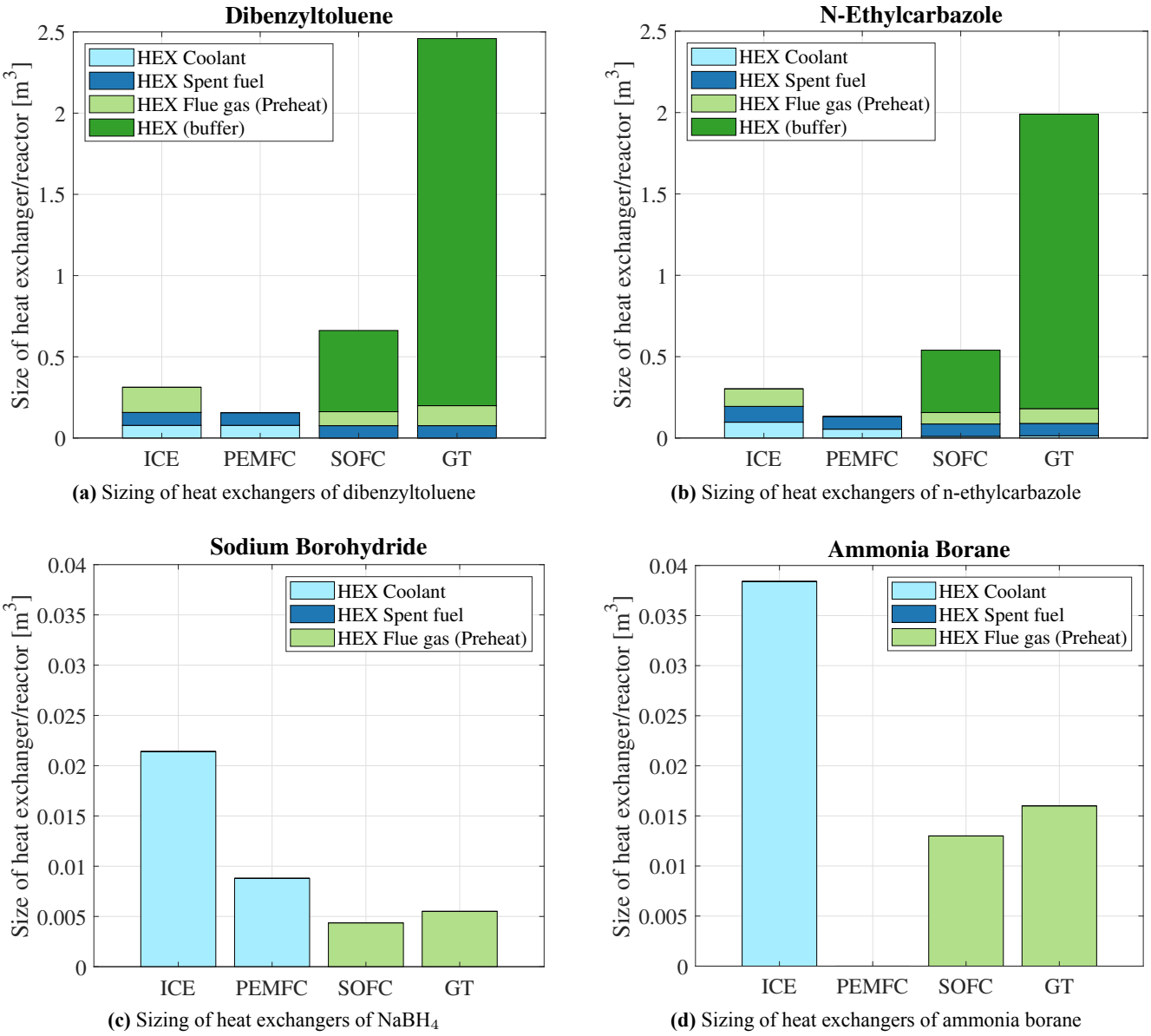

(a) Sizing of heat exchangers of dibenzyltoluene

(b) Sizing of heat exchangers of n-ethylcarbazole

(c) Sizing of heat exchangers of $NaBH_4$

(d) Sizing of heat exchangers of ammonia borane

Figure 7: Sizing of heat exchangers for different hydrogen carriers, additional possible hydrogen heaters are not taken into account

changers, when integrating with an ICE or PEMFC, are significantly smaller than those with a SOFC or GT. However, it should be noted here that the ICE and the PEMFC cannot cover the complete heat requirement of the preheating and dehydrogenation process of the LOHCs. An additional heat source, most likely hydrogen burning, is thus required. This reduces the energy density and efficiency of the system and requires an additional heater. This additional heater also needs to be sized. However, as this is a burner and not a heat exchanger, it is not considered here.

On the other hand, the complete system of heat exchangers required for the SOFC or GT integration can be simulated. Figure 7a shows that heating the buffer fluid results in an extremely large heat exchanger for this system. The large heat demand of the dehydrogenation process can explain this. The complete flue gas flow is required to heat the buffer fluid sufficiently. For both N-ethylcarbazole and dibenzyltoluene, the differences between the gas turbine and the SOFC buffer-fluid heat exchanger are significant. These differences occur due to the mass flow of the flue gas of a gas turbine and SOFC. The mass flows are calculated using equation 4. As the SOFC has a larger temperature difference, the mass flow is consequently less than for the GT, with a smaller temperature difference. Additionally, the SOFC has a higher efficiency and, as visible

in table 2, the overall component of the total available power going to heat is less for an SOFC than for a GT. Thus, combined, the mass flow of an SOFC is much lower than that of a GT, resulting in a smaller heat exchanger. However, figure 7a shows much larger heat exchangers in general, especially visible in the buffer, but also the other heat exchangers (for all energy converters) are larger. This difference occurs because dbt generally requires more heat, both for preheating and dehydrogenating. In figure 7b, a very small, additional heat exchanger is visible, which is required as the spent fuel of NEC should not be used to preheat the fuel at low temperatures. The spent fuel freezes at around 343K and should thus not be cooled down strongly. Thus, a heat exchanger must be added to do the first flue gas cooling step. These heat exchangers are generally very small, approximately 10L.

Knowing the size of the heat exchangers is not the only result of this study. The sequence and amount of heat exchangers is also an important input for ship design. As all the heat exchangers have to be connected to each other and different heat sources, they introduce limitations to the ship's design (Souflis-Rigas et al., 2023). These limitations occur less when using fewer and smaller heat exchangers; the design freedom when incorporating boron-based hydrogen carriers is thus much higher compared to LOHCs.

Reactor

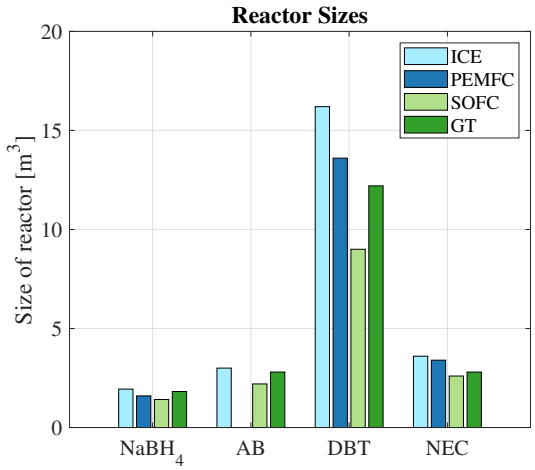

Figure 8: Estimated reactor sizes of different hydrogen carriers for different energy converters

Figure 8 gives an overview of the reactor sizes. The reactor size depends largely on the throughput time. In this case, a throughput time which results in a high conversion rate (>95%) is chosen. The throughput time can be shorter for lower conversion rates. The conversion rate depends on the temperature, catalyst, reaction rate, type of reactor, and more (Brückner et al., 2014; Abdelhamid, 2021). Additionally, catalyst packing influences the volume size. In all of the cases, a packing factor of 0.5 is considered. The throughput time and conversion rate do not depend on the energy converter. The differences for each energy converter, as visible in figure 8, occur due to different mass flows. Higher mass flows with the same throughput time result in a larger reactor size.

Experiments are generally required to calculate conversion rates and throughput times. These conversion rates and throughput times strongly influence the reactor size and the hydrogen release rate. Literature shows this as well. $NaBH_4$, for example, was reported to have throughput times of 1 to 2 hours (Li & Kim, 2012), whereas more recently, throughput times in the order of 20 minutes have been reported (Erat, Bozkurt, & Özer, 2022). Thus, they form an area of very active research, as the hydrogen release rate influences the suitability and usability of a hydrogen carrier. As this area of research is very specialised, we only considered known throughput times with a high conversion rate (Brückner et al., 2014; Qiu, Wu, Wu, Liu, & Huang, 2016; Erat et al., 2022). Figure 8 clearly demonstrates the requirement for low throughput times, as the difference in reactor size is large.

Overview of total required components

Figure 9 gives an overview of the total sum of the size of the required components. Each of the specific components is influenced by several factors, each with its own levels of reliability. Thus, the resulting sum of the sizes is an indication. The reactor size is the main influence of the components' total sizing. This figure clearly shows that the equipment's total size does not differ too much if the throughput time of the reactor is low enough. The relatively large heat exchangers required for NEC and DBT are only relevant if the reactor size is similar to that of $NaBH_4$ and ammonia borane. Even then, the overall sizing of the equipment is similar. The size of the mixing tank required for $NaBH_4$ and ammonia borane is similar to the heat exchangers required for DBT and NEC (except when combining these with a GT, in which case the heat exchangers are significantly larger).

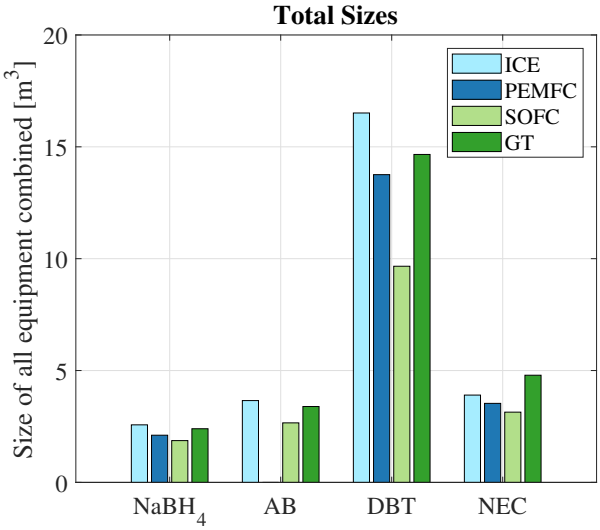

Figure 9: Overview of sizing of all components

CONCLUSION AND RECOMMENDATIONS

The sizing of all relevant components must be known to estimate the possible ship design changes required for incorporating hydrogen carriers as the power source. This research aims to give an overview of all the relevant components and their sizes.

The size of the release reactor is most significant for all hydrogen carriers. Further research on catalysts will hopefully result in shorter throughput times. This research clearly shows the benefit of shorter throughput times, as these strongly influence the reactor sizing. As this reactor has to be placed in a specialised room (due to the release of hydrogen), having an exact size is important. The reactors required for ammonia borane appear slightly larger than those for sodium borohydride reactors. This size largely depends on the throughput time and dehydrogenation rate. The other components, such as heat exchangers and a mixing tank, are significantly smaller than the reactor. The heat exchangers are of such small size that it is unlikely they will influence ship design.

The sizing of heat exchangers is of importance only for LOHCs. The heat exchangers required to heat the buffer fluid are especially large. When no buffer fluid is required, and the main part of heating has to be done using hydrogen, no estimates on equipment size have been made. In general, the heat exchangers required to preheat and, when possible, provide enough heat for the dehydrogenation process of LOHCs are large and numerous. As these heat exchangers need to be in a fixed sequence and use waste heat, they create limitations on the ship design. Additionally, all of the equipment for DBT is larger than that for NEC.

All in all, the boron-based carriers pose fewer limitations to ship design. The required equipment is smaller and less numerous, even though it is still in a fixed sequence. In all cases except for the PEMFC, only three components are necessary: a mixing tank, a single heat exchanger and a reactor vessel. When a PEMFC is used, a small hydrogen burner is also required. For LOHCs, more and larger components are needed. The only setups in which no hydrogen burner is required need at least 3 (for DBT) or 4 (for NEC) heat exchangers. Besides these, a reactor is also required.

To design ships using hydrogen carriers, knowing the amount of components and their sizing is imperative. This research has given an overview of all required components and estimated the sizing of each of these components. This is the first step in designing zero-emission ships powered by hydrogen carriers.

CONTRIBUTION STATEMENT

E.S. van Rheenen: Conceptualization; data curation; methodology; visualisation; writing – original draft. **J.T. Padding:** conceptualization; methodology; supervision; writing – review and editing. **A.A. Kana:** conceptualization; methodology; supervision; writing – review and editing. **K. Visser:** conceptualization; methodology; supervision; writing – review and editing.

ACKNOWLEDGEMENTS

This work was supported by the project SH2IPDRIVE, which has received funding from the Ministry of Economic Affairs and Climate Policy, RDM regulation, carried out by the Netherlands Enterprise Agency (RvO).

REFERENCES

Abdelhamid, H. N. (2021). A review on hydrogen generation from the hydrolysis of sodium borohydride. *International Journal of Hydrogen Energy*, *46*(1), 726-765. doi: 10.1016/j.ijhydene.2020.09.186

Andrieux, J., Laversenne, L., Krol, O., Chiriac, R., Bouajila, Z., Tenu, R., … Goutaudier, C. (2012). Revision of the nabo2–h2o phase diagram for optimized yield in the h2 generation through nabh4 hydrolysis. *International Journal of Hydrogen Energy*, *37*(7), 5798-5810. (XII International Symposium on Polymer Electrolytes: New Materials for Application in Proton Exchange Membrane Fuel Cells) doi: 10.1016/j.ijhydene.2011.12.106

Asif, F., Hamayun, M. H., Hussain, M., Hussain, A., Maafa, I. M., & Park, Y.-K. (2021). Performance analysis of the perhydro-dibenzyl-toluene dehydrogenation system—a simulation study. *Sustainability*, *13*(11). doi: 10.3390/su13116490

Brückner, N., Obesser, K., Bösmann, A., Teichmann, D., Arlt, W., Dungs, J., & Wasserscheid, P. (2014, 01). Evaluation of industrially applied heat-transfer fluids as liquid organic hydrogen carrier systems. *ChemSusChem*, *7*. doi: 10.1002/cssc.201300426

Cengel, Y. A., & Ghajar, A. J. (2014). *Heat and mass transfer: Fundamentals and applications* (5th ed.). New York, NY: McGraw-Hill Professional.

Chandra, M., & Xu, Q. (2007, 5). Room temperature hydrogen generation from aqueous ammonia-borane using noble metal nano-clusters as highly active catalysts. *Journal of Power Sources*, *168*, 135-142. doi: 10.1016/J.JPOWSOUR.2007.03.015

Crapse, K., & Kyser, E. (2011). *Literature review of boric acid solubility data* (Tech. Rep.). Savannah River National Laboratory (SRNL). doi: 10.2172/1025802

de Vos, P., de van der Schueren, T., Los, S., & Visser, K. (2022). Effective naval power plant design space exploration.. doi: 10.24868/10680

Demirci, U. B. (2020). Ammonia borane: An extensively studied, though not yet implemented, hydrogen carrier. *Energies*, *13*(12). doi: 10.3390/en13123071

Dimitriou, P., & Tsujimura, T. (2017). A review of hydrogen as a compression ignition engine fuel. *International Journal of Hydrogen Energy*, *42*(38), 24470-24486. doi: 10.1016/j.ijhydene.2017.07.232

Erat, N., Bozkurt, G., & Özer, A. (2022). Co/cuo–nio–al2o3 catalyst for hydrogen generation from hydrolysis of nabh4. *International Journal of Hydrogen Energy*, *47*(58), 24255-24267. (Hydrogen Sourced from Renewables and Clean Energy: Feasibility of Large-scale Demonstration Projects) doi: 10.1016/j.ijhydene.2022.05.178

Fogler, H. S. (2016). *Elements of chemical reaction engineering*. Prentice Hall.

Gohary, M. M. E., & Seddiek, I. S. (2013, 3). Utilization of alternative marine fuels for gas turbine power plant onboard ships. *International Journal of Naval Architecture and Ocean Engineering*, *5*, 21-32. doi: 10.2478/IJNAOE-2013-0115

Halseid, R., Vie, P. J., & Tunold, R. (2006). Effect of ammonia on the performance of polymer electrolyte membrane fuel cells. *Journal of Power Sources*, *154*(2), 343-350. (Selected papers from the Ninth Ulm Electrochemical Days) doi: 10.1016/j.jpowsour.2005.10.011

Haynes, W. M. (Ed.). (2011). *CRC handbook of chemistry and physics, 92nd edition* (92nd ed.). Boca Raton, FL: CRC Press.

Kemp, I. C., & Shiun Lim, J. (2020). Chapter 3 - key concepts of pinch analysis. In I. C. Kemp & J. Shiun Lim (Eds.), *Pinch analysis for energy and carbon footprint reduction (third edition)* (Third Edition ed., p. 35-61). Butterworth-Heinemann. doi: 10.1016/B978-0-08-102536-9.00003-5

Kojima, Y. (2019, 7). Hydrogen storage materials for hydrogen and energy carriers. *International Journal of Hydrogen Energy*, *44*, 18179-18192. doi: 10.1016/J.IJHYDENE.2019.05.119

Kwak, Y., Kirk, J., Moon, S., Ohm, T., Lee, Y. J., Jang, M., … Kim, Y. (2021, 7). Hydrogen production from homocyclic liquid organic hydrogen carriers (lohcs): Benchmarking studies and energy-economic analyses. *Energy Conversion and Management*, *239*, 114124. doi: 10.1016/J.ENCONMAN.2021.114124

Lee, S., Kim, T., Han, G., Kang, S., Yoo, Y. S., Jeon, S. Y., & Bae, J. (2021, 10). Comparative energetic studies on liquid organic hydrogen carrier: A net energy analysis. *Renewable and Sustainable Energy Reviews*, *150*. doi: 10.1016/j.rser.2021.111447

Li, Q., & Kim, H. (2012). Hydrogen production from nabh4 hydrolysis via co-zif-9 catalyst. *Fuel Processing Technology*, *100*, 43-48. doi: 10.1016/j.fuproc.2012.03.007

Müller, K., Stark, K., Emel'yanenko, V. N., Varfolomeev, M. A., Zaitsau, D. H., Shoifet, E., … Arlt, W. (2015). Liquid organic hydrogen carriers: Thermophysical and thermochemical studies of benzyl- and dibenzyl-toluene derivatives. *Industrial & Engineering Chemistry Research*, *54*(32), 7967-7976. doi: 10.1021/acs.iecr.5b01840

Niermann, M., Beckendorff, A., Kaltschmitt, M., & Bonhoff, K. (2019, 3). Liquid organic hydrogen carrier (lohc) – assessment based on chemical and economic properties. *International Journal of Hydrogen Energy*, *44*, 6631-6654. doi: 10.1016/j.ijhydene.2019.01.199

Pawling, R., Bucknall, R., & Greig, A. (2022). Considerations for future fuels in naval vessels. *Conference Proceedings of INEC*. doi: 10.24868/10676

Preuster, P., Fang, Q., Peters, R., Deja, R., Nguyen, V. N., Blum, L., … Wasserscheid, P. (2018, 1). Solid oxide fuel cell operating on liquid organic hydrogen carrier-based hydrogen – making full use of heat integration potentials. *International Journal of Hydrogen Energy*, *43*, 1758-1768. doi: 10.1016/J.IJHYDENE.2017.11.054

Qiu, X., Wu, X., Wu, Y., Liu, Q., & Huang, C. (2016). The release of hydrogen from ammonia borane over copper/hexagonal boron nitride composites. *RSC Adv.*, *6*, 106211-106217. doi: 10.1039/C6RA24000C

Reay, D., Ramshaw, C., & Harvey, A. (2008). Chapter 4 - compact and micro-heat exchangers. In *Process intensification* (p. 77-101). Oxford: Butterworth-Heinemann. doi: 10.1016/B978-0-7506-8941-0.00005-5

Rosado, D. M., Chavez, S. R., & de Carvalho Jr, J. (2019, 10). Determination of global efficiency without/with supplementary burning of a thermoelectric plant with combined cycle of natural gas.. doi: 10.26678/ABCM.COBEM2019.COB2019-0024

Sanyal, U., Demirci, U. B., Jagirdar, B. R., & Miele, P. (2003). Hydrolysis of ammonia borane as a hydrogen source: Fundamental issues and potential solutions towards implementation. *ChemSusChem*, *4*. doi: 10.1002/cssc.201100318

Shah, R. K., & Sekulić, D. P. (2003). *Fundamentals of heat exchanger design*. John Wiley & Sons.

Souflis-Rigas, A., Pruyn, J., & Kana, A. (2023). Establishing the influence of methanol fuelled power propulsion and energy systems on ship design. In *Proceedings of moses2023 conference.* doi: 10.59490/moses.2023.658

Stark, K., Emelyanenko, V. N., Zhabina, A. A., Varfolomeev, M. A., Verevkin, S. P., Müller, K., & Arlt, W. (2015, 8). Liquid organic hydrogen carriers: Thermophysical and thermochemical studies of carbazole partly and fully hydrogenated derivatives. *Industrial and Engineering Chemistry Research*, *54*, 7953-7966. doi: 10.1021/ACS.IECR.5B01841

Stephens, F. H., Pons, V., & Tom Baker, R. (2007). Ammonia–borane: the hydrogen source par excellence? *Dalton Trans.*, 2613-2626. doi: 10.1039/B703053C

Teichmann, D., Stark, K., Müller, K., Zoettl, G., Wasserscheid, P., & Arlt, W. (2012, 09). Energy storage in residential and commercial buildings via liquid organic hydrogen carriers (lohc). *Energy Environ. Sci.*, *5*, 9044-9054. doi: 10.1039/C2EE22070A

van Rheenen, E. S., Padding, J. T., Slootweg, J. C., & Visser, K. (2023). Hydrogen carriers for zero-emission ship propulsion using pem fuel cells: an evaluation. *Journal of Marine Engineering & Technology*, 1-18. doi: 10.1080/20464177.2023.2282691

van Rheenen, E. S., Padding, J. T., & Visser, K. (2023). A 0d model for the comparative analysis of hydrogen carriers in ship's integrated energy systems. In *Proceedings of moses2023 conference.*

van Veldhuizen, B., van Biert, L., Amladi, A., Woudstra, T., Visser, K., & Aravind, P. (2023). The effects of fuel type and cathode off-gas recirculation on combined heat and power generation of marine sofc systems. *Energy Conversion and Management*, *276*, 116498. doi: 10.1016/j.enconman.2022.116498

Wang, X., Sun, B.-G., & Luo, Q.-H. (2019, 2). Energy and exergy analysis of a turbocharged hydrogen internal combustion engine. *International Journal of Hydrogen Energy*, *44*, 5551-5563. doi: 10.1016/J.IJHYDENE.2018.10.047

Ye, L., Li, D., Dong, Y. P., Xu, B., & Zeng, D. (2020, 5). Measurement of specific heat capacity of nabo2(aq) solution and thermodynamic modeling of nabo2 + h2o, nabo2 + nacl + h2o, and nabo2 + na2so4 + h2o systems. *Journal of Chemical and Engineering Data*, *65*, 2548-2557. doi: 10.1021/ACS.JCED.9B01182

Zhang, J., Fisher, T. S., Gore, J. P., Hazra, D., & Ramachandran, P. V. (2006, 12). Heat of reaction measurements of sodium borohydride alcoholysis and hydrolysis. *International Journal of Hydrogen Energy*, *31*, 2292-2298. doi: 10.1016/J.IJHYDENE.2006.02.026

Zhao, L., Brouwer, J., James, S., Siegler, J., Peterson, E., Kansal, A., & Liu, J. (2017). Dynamic performance of an in-rack proton exchange membrane fuel cell battery system to power servers. *International Journal of Hydrogen Energy*, *42*(15), 10158-10174. doi: 10.1016/j.ijhydene.2017.03.004